



Blue/green/red colour emitting up-conversion phosphors coupled C-TiO₂ composites with UV, visible and NIR responsive photocatalytic performance

Xiaoyong Wu, Shu Yin*, Qiang Dong, Tsugio Sato

Institute of Multidisciplinary Research for Advanced Materials, Tohoku University, 2-1-1, Katahira, Aoba-ku, Sendai 980-8577, Japan



ARTICLE INFO

Article history:

Received 29 December 2013

Received in revised form 6 February 2014

Accepted 13 March 2014

Available online 21 March 2014

Keywords:

Up-conversion phosphor

C-TiO₂

Composites

Infrared light

Photocatalytic activity

ABSTRACT

The composites of C-TiO₂ coupled with blue, green and red of three colours emitting up-conversion phosphors have been prepared by a simple calcination assisted solvothermal method. The composites of the narrow band gap of C-TiO₂ and the unique optical property of up-conversion phosphors enabled to absorb UV, visible and NIR lights simultaneously to proceed photocatalytic reactions effectively. The photocatalytic activities of the composites were evaluated not only for the degradation of RhB solution under NIR light irradiation but also for the destruction of continuous NO gas under the irradiation of UV, visible LEDs and infrared laser. According to the photocatalytic results, the calculated photonic efficiency of infrared light induced photocatalytic activity of samples was much higher than those of UV and visible light responsive ones. Furthermore, the green light emitting up-conversion phosphor coupled C-TiO₂ composite presented the superior photocatalytic performance over blue and red ones.

© 2014 Elsevier B.V. All rights reserved.

1. Introduction

In recent years, air and water contamination has become more and more serious all over the world. Photocatalysis as a green chemistry method for pollution treatment has drawn lots of attention [1–4]. Although a great amount of novel compounds with various photocatalytic performances have been developed until now [5–7], TiO₂ is still the most promising photocatalyst due to its chemical stability, environmentally friendly, high oxidative power and low cost [8–10]. However, it can only be activated by UV light because of the large band gap of ca. 3.2 eV. It is well acknowledged that the UV light just accounts for 5% of solar light, while the residual 45% and 50% of solar light are made up of visible light and near-infrared (NIR) light, respectively [11,12]. In order to extend the absorption ability of TiO₂ to the visible-light region, many strategies, such as dye sensitizing [13,14], heterostructure [15,16], ion doping [17–19], etc. have been developed. As for NIR light induced photocatalytic utilization, two dominant methods have been proposed. The one way is the doping of TiO₂ with lanthanide ion, which can emit UV or visible light by directly absorbing NIR by the multi-step excitation mechanism. Obregón et al. [20] reported an erbium doped TiO₂ particles prepared by a surfactant free hydrothermal method.

The Er-TiO₂ presented nice photoactivities for the degradation of phenol under sun-like excitation, owing to the improved NIR light absorption and NIR-UV up-conversion luminescence contribution induced by Er doping. However, the self-induced up-conversion luminescence by TiO₂ substrate is very poor and not efficient. In this case, the NIR light cannot be effectively used for photocatalysis. The other method is the formation of composite between the high performance up-conversion phosphors (lanthanide-doped NaYF₄, YF₃, Y₂O₃, YOF, etc.) and photocatalyst substrates. For this type of composite, the NIR light cannot be directly utilized for photocatalysis but is first absorbed by the up-conversion phosphor to emit some UV or visible lights, and then the emitted UV or visible lights are reabsorbed by the coexisted photocatalyst to proceed photocatalytic reactions. In order to effectively utilize the emitted lights from up-conversion phosphor for the photocatalysis, one of the key points is the nice overlap of the NIR light excited emission spectrum of the up-conversion phosphor with the absorption spectrum of the photocatalyst. Qin group first studied NIR-responsive photocatalysis of TiO₂ by combining it with YF₃:Yb, Tm or NaYF₄:Yb, Tm [21,22]. It was reported that the emitted UV light from YF₃:Yb, Tm or NaYF₄:Yb, Tm could be effectively used by TiO₂ for photocatalytic reaction under the irradiation of NIR light. There were also some other reports on NIR light induced composites [23–25]. Recently, our group [26] also prepared a NaYF₄:Yb, Er/C-TiO₂ composite, which was able to be excited by UV, visible and NIR lights effectively, producing corresponding nice photocatalytic activity due

* Corresponding author.

E-mail address: shuyin@tagen.tohoku.ac.jp (S. Yin).

to the excellent absorption capability of C-TiO₂ and outstanding optical property of NaYF₄:Yb, Er up-conversion phosphor. As we all known, different colours emitting up-conversion phosphors can present big difference in the photoluminescence property. In this case, a systematic investigation about the different colours emitting up-conversion phosphors (blue, green, red colours) coupled photocatalyst composites would be meaningful to understand the effect of up-conversion phosphors on the photocatalytic activity of photocatalysts deeply. Nevertheless, to the best of our knowledge, there is still no research about the different colours emitting up-conversion phosphors combined photocatalyst composites.

On the other hand, in order to utilize blue, green, red colour emitting up-conversion phosphors for NIR induced composite photocatalyst, a suitable photocatalyst substrate, which have a nice photocatalytic response in the range of blue, green and red lights, is strongly required. According to our previous results [26], the C doped TiO₂ [27] (C-TiO₂) by replacing the oxygen site with C element in the TiO₂ lattice shows excellent visible light absorption ability up to 800 nm, covering the whole visible light range from blue light to red light. Furthermore, the modified or coupled C-TiO₂ presents the similar excellent photocatalytic performance in the long wavelengths range until 800 nm, indicating its higher efficiency than that of commercial P25. [26,27] So the C doped TiO₂ would also be a promising photocatalyst substrate for various colours emitting up-conversion phosphors coupled composites.

For the purpose of practical application, a photonic efficiency of energy conversion from NIR light to the photocatalytic performance between up-conversion phosphors and photocatalyst substrate is essential. In addition, it would be better that the photocatalytic testing was carried out not only for pollutant aqueous solution degradation but also toxic gas destruction. Therefore, based on the above mentioned requirements, three types of blue, green, red colour emitting up-conversion phosphors coupled C-TiO₂ composites have been first prepared by a simple calcination assisted solvothermal method in this work, and the photocatalytic performances of them were evaluated for the destruction of NO_x gas and rhodamine B (RhB) solution with the induction of UV, visible and NIR lights, indicating their benefit for practical application in the area of air purification and water cleaning. Besides, the photocatalytic stability and the effect of the power of irradiation light on the photocatalytic activity of composites have also been investigated. More importantly, the apparent photonic efficiency about the photocatalytic ability of the composite photocatalysts under the irradiation of UV, visible and NIR lights were calculated. They are essential for understanding the effect of up-conversions and near infrared light on the photocatalytic performance of semiconductors. The proposed method for NIR light utilization along with those of UV and visible lights by coupling different colours up-conversion phosphors with high performance of C-TiO₂ or other effective substrate probably have promising potential for the dye sensitized solar cell.

2. Experimental

2.1. Sample preparation

The blue, green and red colour emitting up-conversion phosphors coupled C-TiO₂ composites were prepared by a simple calcination assisted solvothermal method. The blue colour (Yb, Tm)-NaYF₄ (named B-UP), green colour (Yb, Er)-NaYF₄ (named G-UP) and red colour (Yb, Er)-Y₂O₃/YOF (named R-UP) up-conversion phosphors used in this experiment were purchased from Shanghai Keyan Phosphor Technology Co., Ltd (China). These three commercial up-conversion phosphors were mixed with C-TiO₂ by a weight ratio of 1:1 and were denoted as (1:1) @B-UP/C-TiO₂, (1:1)

@G-UP/C-TiO₂ and (1:1) @R-UP/C-TiO₂, respectively. In a typical synthesis process of (1:1) @ B-UP/C-TiO₂ composite, after dispersing an appropriate amount of B-UP particles in 20 mL ethanol with continuous stirring for 60 min, 0.6 mL titanium tetra-*n*-butoxide was added dropwise with 30 min magnetic stirring. Subsequently, 10.5 mL ethanol/water (10:0.5) mixed solution was introduced dropwise, and the suspension solution was stirred for 60 min before transferring into a 100 mL Teflon-lined stainless steel autoclave and solvothermal treatment at 190 °C for 2 h. Finally, the products were recovered by centrifuge, followed by washing, drying and calcination at 265 °C for 1 h in an ambient condition. The pure C-TiO₂ was fabricated without the addition of commercial up-conversion phosphors. The composites of (1:1) @G-UP/C-TiO₂, and (1:1) @R-UP/C-TiO₂ were also fabricated by similar process using corresponding up-conversion phosphors.

2.2. Characterization

The crystalline phases of the products were identified by X-ray diffraction analysis (XRD, Bruker AXS D2 Phaser) using graphite-monochromized Cu K α radiation. The UV-vis diffuse reflectance spectra (DRS) were measured using an UV-vis spectrophotometer (Shimadzu, UV-2450). The BET specific surface areas were determined by the BJH method (Quantachrome Instruments, NOVA4200e). The size, shape and element mapping of the composites were observed by transmission electron microscopy (TEM, JEOLJEM-2010) and high resolution transmission electron microscopy (HRTEM) (FE-TEM, JEM-2100F). The surface composition and binding energy of the samples were determined by X-ray photoelectron spectroscopy (XPS, Perkin Elmer PHI 5600). The shift of the binding energy owing to the relative surface charging was corrected using the C 1s level at 284.6 eV as an internal standard and Ar⁺ sputtering was employed to clean the surface of samples. Photoluminescence (PL) spectra of specimens were measured by a spectrofluorometer (Shimadzu RF-5300P).

2.3. Photocatalytic activity tests

The photocatalytic activities of composites were investigated by evaluating the decomposition of NO_x (DeNO_x) in a flow type reactor under irradiation of different wavelengths of LEDs and NIR laser (see Supplementary Fig. A.1) at room temperature, while the detailed testing parameters were summarized in Supplementary Table A.1. The sample powders were spread in the hollow (20 mm × 16 mm × 0.5 mm) of a glass plate and then set at the bottom center of the reactor (373 cm³ of internal volume) in which a 1:1 mixed gas of air and nitrogen balanced 2 ppm of NO was flowed at the rate of 200 cm³ min⁻¹. The composites were kept in the dark for 30 min to reach the adsorption and desorption equilibrium of NO gas. After that, the irradiation light source was turned on to excite the sample for 10 min and then turned off to make the concentration of NO recover to the original level for another 10 min, i.e., the measuring time for each sample under each light source was 20 min [19]. In this testing process, the photocatalytic performance of NO gas destruction was determined by checking the change of NO gas concentration in the irradiation time instead of other deNO_x products. The concentration of NO was monitored by a NO_x analyzer (Yanaco, ECL-88A) continuously. Besides, the testing temperature was kept at ca. 25 °C by using an electric fan and air conditioner.

The photocatalytic activity of composites was also evaluated for the degradation of RhB solution under the irradiation of 980 nm NIR laser at the ambient temperature. After the addition of 0.10 g of sample powder into a 50 mL of 10⁻⁵ mol L⁻¹ RhB solution, the solution was stirred for 2 h in the dark to reach the adsorption-desorption equilibrium of RhB prior to irradiation of the NIR laser. 5 mL suspensions were withdrawn at the desired

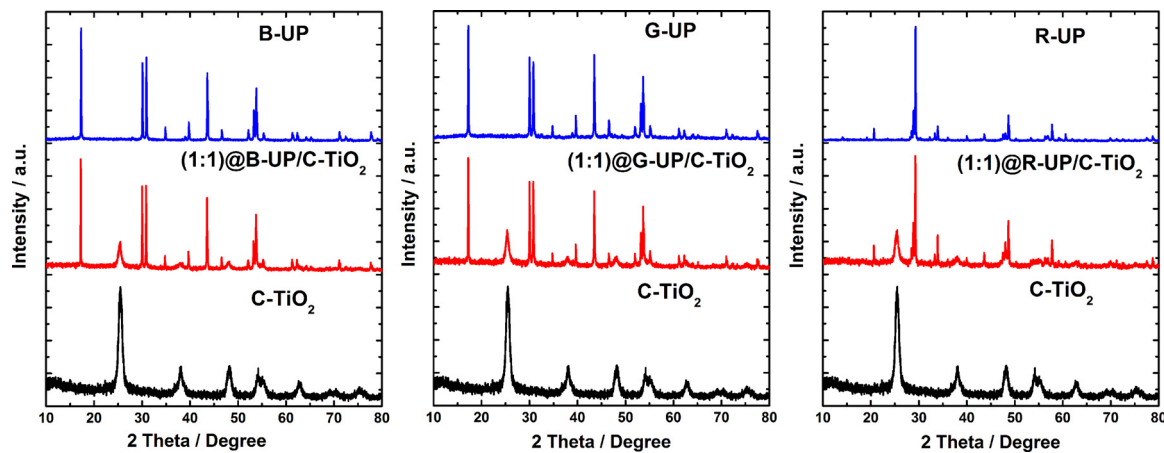


Fig. 1. XRD patterns of C-TiO₂, B-UP, G-UP, R-UP and the composites (1:1)@B-UP/C-TiO₂, (1:1)@G-UP/C-TiO₂ and (1:1)@R-UP/C-TiO₂.

illumination time intervals, and the particles were removed by centrifugation to monitor the concentration of RhB by recording the maximum absorbance of RhB at 553 nm with the UV-vis spectrophotometer.

3. Results and discussion

Fig. 1 shows the XRD patterns of C-TiO₂, three kind commercial up-conversion phosphors and the corresponding composites. It could be obviously seen that C-TiO₂ presented the pure anatase phase (JCPDS file no. 21-1272) and no other impurity peaks or phases were observed. After coupling C-TiO₂ with B-UP, G-UP, R-UP by the solvothermal method, the diffraction peaks belonged to C-TiO₂ and various up-conversion phosphors were observed, implying that the composites had been successfully formed without changing the crystallinity of C-TiO₂ and commercial up-conversion phosphors. The representative SEM images of C-TiO₂, G-UP, composites (1:1)@B-UP/C-TiO₂, (1:1)@G-UP/C-TiO₂ (1:1)@R-UP/C-TiO₂ and the representative TEM image, element mappings of composite (1:1)@G-UP/C-TiO₂ are also illustrated in Figs. A.2 and A.3, respectively. It is apparent that the C-TiO₂ with small particle size successfully covered on the surface of the large particle of commercial up-conversion phosphors in the composite. In addition, the C-TiO₂ possessed fine particle size of ca. 10 nm and large specific surface area of 124.3 m² g⁻¹, which was much higher than that of commercial P25 (50.2 m² g⁻¹). After combining with B-UP, G-UP and R-UP, the specific surface areas of the composite decreased to about 66.7, 69.2 and 74.5 m² g⁻¹, respectively, owing to the large particle size (about 2 μm in diameter) of the up-conversion phosphors together with its small specific surface area of about several m² g⁻¹.

The DRS of C-TiO₂ particle and (1:1)@B-UP/C-TiO₂, (1:1)@G-UP/C-TiO₂, (1:1)@R-UP/C-TiO₂ composites are illustrated in Fig. 2. It is explicit that C-TiO₂ presented nice UV and visible lights absorption but no NIR light absorption. When C-TiO₂ was combined with up-conversion phosphors, the composites not only displayed improved visible lights absorption up to 800 nm, covering the whole blue, green and red lights range, but also represented a small NIR light absorption band around 980 nm. The increase in the visible light absorption might be owing to the increased C doping contents in TiO₂, and the absorption of NIR light might be corresponded to the absorption ability of Yb³⁺ ions in the up-conversion phosphors [28,29]. It means that the prepared composites can be excited by UV, visible and NIR lights simultaneously.

Fig. 3 represents the DRS, PL spectra, visual emitting map of three composites together with the PL spectra of up-conversion

phosphors of B-UP, G-UP and R-UP monitored by 980 nm laser. It is obvious in Fig. 3(a)–(c) that (1:1)@B-UP/C-TiO₂, (1:1)@G-UP/C-TiO₂ and (1:1)@R-UP/C-TiO₂ composites displayed the good visual blue, green, red colour emissions, respectively, under the irradiation of 980 nm laser. Furthermore, the DRS and PL spectra of all composites demonstrated the nice overlap, indicating that the up-conversion emitted blue, green and red lights could be well reabsorbed by the C-TiO₂ coexisted in the composite. Such reabsorption of up-conversion emitted lights by C-TiO₂ photocatalyst in composites could be confirmed by Fig. 3(d). The up-conversion phosphors B-UP, G-UP and R-UP revealed the high blue, green and red colour emission peaks situated at about 453, 538 and 662 nm, respectively, where the G-UP exhibited much stronger emission intensity than those of the B-UP and R-UP. After coupling the C-TiO₂, the intensity of up-conversion emission decreased dramatically, due to the absorption by C-TiO₂. The G-UP combined composite still displayed the strongest emission intensity among the three composites which well agreed with the visual emitting maps in Fig. 3(a)–(c). Compared with the emission intensity of pure up-conversion phosphors, the intensity of blue colour in (1:1)@B-UP/C-TiO₂ composite reduced about 89%, green colour in (1:1)@G-UP/C-TiO₂ composite about 75% and red colour in (1:1)@R-UP/C-TiO₂ composite about 62%, mainly due to the reabsorption by C-TiO₂ in the composites.

The XPS analysis was also employed to check the status of C in the TiO₂ crystal. Fig. 4 exhibited the XPS spectra of C 1s for the C-TiO₂ particle, (1:1)@B-UP/C-TiO₂, (1:1)@G-UP/C-TiO₂ and (1:1)@R-UP/C-TiO₂ composites after Ar⁺ sputtering to clean the

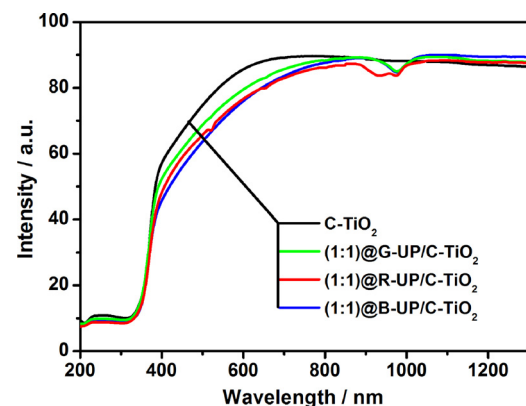


Fig. 2. DRS of samples C-TiO₂, (1:1)@B-UP/C-TiO₂, (1:1)@G-UP/C-TiO₂ and (1:1)@R-UP/C-TiO₂. (For interpretation of the references to color in this figure legend, the reader is referred to the web version of this article.)

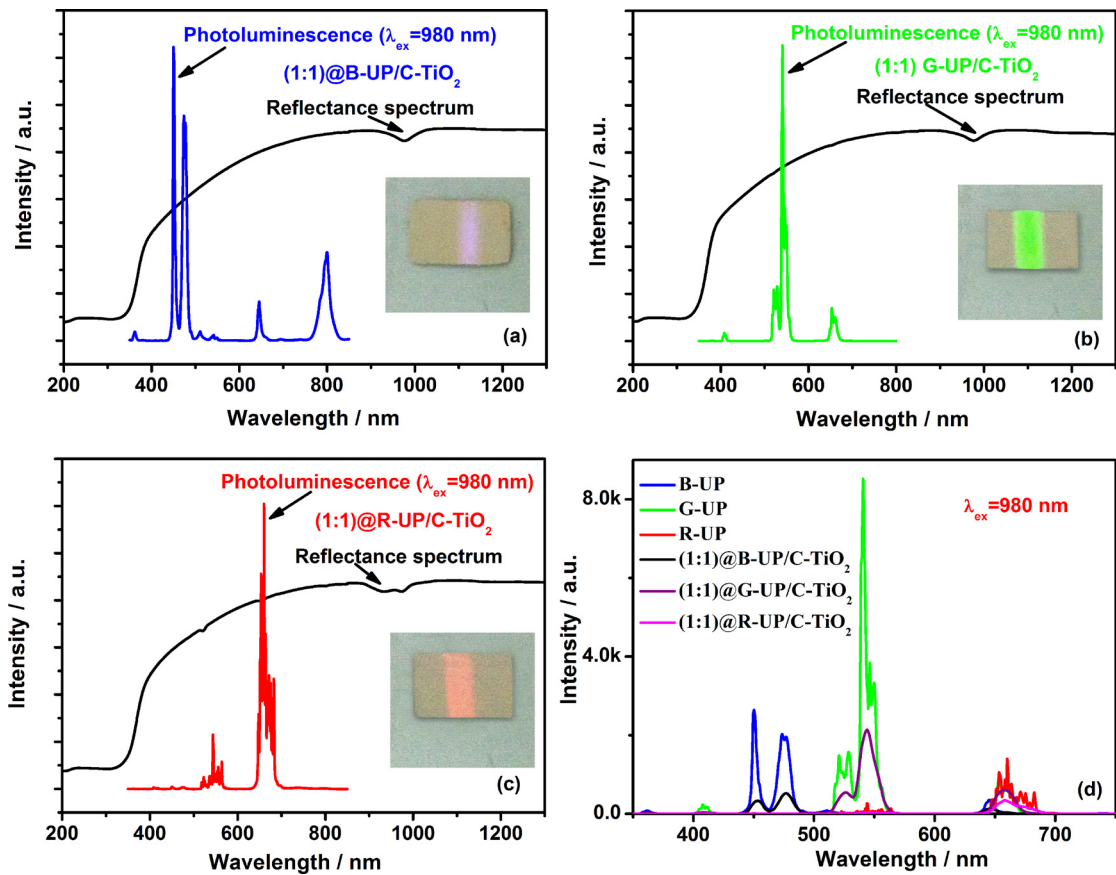


Fig. 3. DRS, PL spectra and visual emitting map of composites (1:1) B-UP/C-TiO₂ (a), (1:1)@ G-UP/C-TiO₂ (b), (1:1)@R-UP/C-TiO₂ (c) and PL spectra of B-UP, G-UP, R-UP and three composites with the excitation of 980 nm (d). (For interpretation of the references to color in this figure legend, the reader is referred to the web version of this article.)

contamination on the surface of the samples. All samples presented three peaks located at 285.6, 284.6 and 282.0 eV, respectively, but the relative peak intensity was varied. The peak situated at 284.6 eV was belonged to the adventitious carbon species and the 285.6 eV

peak was assigned to the elemental carbon which has the same binding energy as that of carbon in the graphite intercalation compound [5,30]. Furthermore, the peak lied at 282.0 eV was attributed to the binding energy of C-Ti bond, indicating that the C was doped into the TiO₂ crystal lattice by replacing the O site [31,32]. However, the relative peak intensities of 282.0 eV for these four samples were different, and the calculated contents of doped C in the samples, C-TiO₂ (1:1)@B-UP/C-TiO₂, (1:1)@G-UP/C-TiO₂ and (1:1)@R-UP/C-TiO₂ composites, were about 0.19, 0.26, 0.24 and 0.25 at%, respectively. The doped C in the samples could introduce some impurity C energy levels into the position above the valence band of TiO₂, finally leading to the narrowed band gap and corresponding improved visible light absorption capability [31–33].

Fig. 5 shows the deNO_x capability of C-TiO₂, (1:1)@B-UP/C-TiO₂, (1:1)@G-UP/C-TiO₂, (1:1)@R-UP/C-TiO₂ and commercial P25 under the excitation of different wavelengths of LED lights and 980 nm NIR laser. As seen in Fig. 5(a)–(c), it is evident that three up-conversion phosphors displayed no obvious NO_x destruction capability regardless of the irradiation source due to the larger particle size and poor visible light absorption ability, while C-TiO₂ represented the nice deNO_x performance and about 6.2%, 23.2%, 28.3%, 32.9% of NO gas were decomposed under the irradiation of LED lights of 627 nm, 530 nm, 445 nm, 390 nm, respectively. As expected, there was no NIR light induced photocatalytic activity for C-TiO₂, because of non-absorption ability of C-TiO₂ in the NIR light range. When C-TiO₂ was combined with up-conversion phosphors, the composites displayed deNO_x ability. More interesting, the composites showed much enhanced red light driven NO_x decomposition performance in compare with that of C-TiO₂. This positive phenomenon was mainly attributed to the increased light absorption ability of C-TiO₂ in the range of visible light (shown in Fig. 2), due to the increased

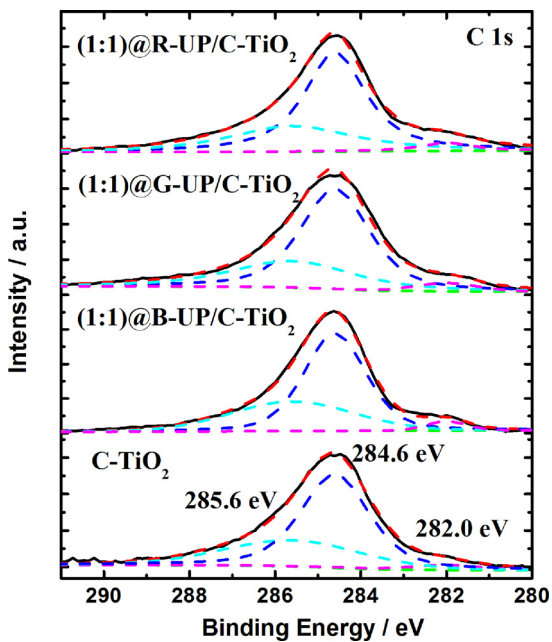


Fig. 4. XPS spectra of C 1s for C-TiO₂, (1:1)@B-UP/C-TiO₂, (1:1)@G-UP/C-TiO₂ and (1:1)@R-UP/C-TiO₂.

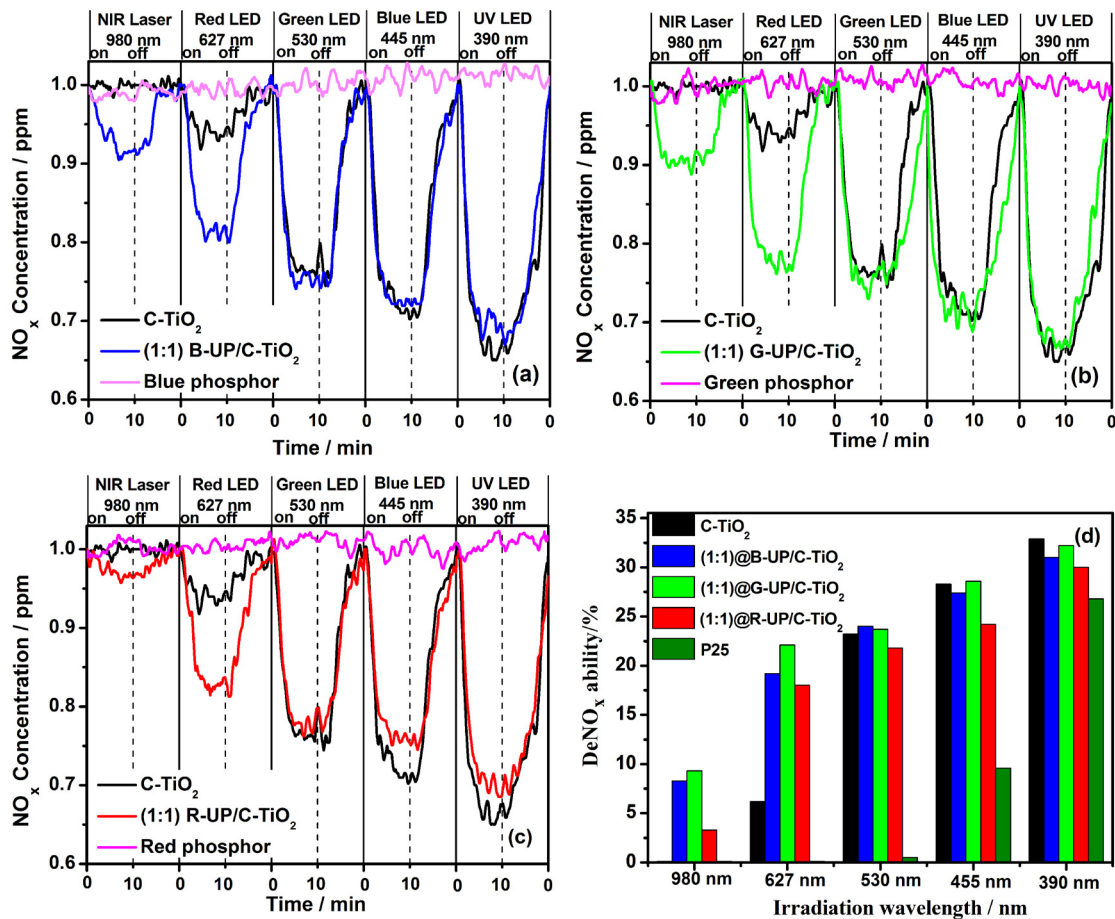


Fig. 5. NO_x destruction activities of C-TiO₂, (1:1)@B-UP/C-TiO₂, (1:1)@G-UP/C-TiO₂, (1:1)@R-UP/C-TiO₂ and P25 under the irradiation of different wavelengths of lights.

C doping content in TiO₂ after solvothermal coupling with up-conversion phosphors in comparison with that of pure C-TiO₂ as shown in Figs. 2 and 4. The detailed reason for increased C doping content in TiO₂ after coupling with up-conversion phosphors was still unclear and would be our next work. However, similar result was also observed in our previous works when the C-TiO₂ combined with other doping ion [32]. With the increase of the whole range of visible light absorption capability for up-conversion phosphors coupled C-TiO₂, only red light induced photocatalytic performance was subsequently increased but no significant change for blue and green lights responsive ones. This abnormal result was probably assigned to the reason that the blue and green lights induced deNO_x ability of pure C-TiO₂ was much higher than that of red light driven one. Although the blue, green and red lights absorption property of up-conversion phosphors combined C-TiO₂ were all enhanced compared with that of pure C-TiO₂, the blue and green lights induced deNO_x ability probably have almost arrived at its saturation and further increased light absorption ability to some extent would be not so effective for the deNO_x performance in contrast to that of poor red light responsive one. The corresponding NO gas degradation ability of the prepared samples and P25 are summarized in Fig. 5(d). It could be explicitly seen that all samples exhibited excellent deNO_x performance superior to P25 even under the irradiation of UV light. Besides, the P25 employed in this work exhibited some of blue light induced deNO_x ability and even a few green light responsive one. For the blue light driven photocatalytic activity of P25, it was probably owing to some impurity contaminations in the commercial P25 products, which finally lead to the visible light induced photocatalytic activity of P25. Similarly, the visible light induced photocatalytic property of P25 was

also observed in many others' works [34,35]. About the very poor green light induced activity of P25, it should be owing to the deviation of testing since sometimes even if no catalyst was employed, similar limited values could be observed [36]. In addition, the (1:1)@G-UP/C-TiO₂ composite emerged the best NIR light induced photocatalytic ability with about 9.3% of NO destruction, following by the (1:1)@B-UP/C-TiO₂ composite with 8.3% and (1:1)@R-UP/C-TiO₂ composite with 3.3%. The reason for the highest NIR light induced deNO_x ability of (1:1)@G-UP/C-TiO₂ composite might be discussed as follows. Although the composites showed higher blue light absorption ability than those of green and red lights (as seen in Fig. 2), the green colour emitting up-conversion phosphor G-UP displayed much stronger emission intensity compared with those of blue and red colours emitting up-conversion phosphors (as exhibited in Fig. 3(d)) under the excitation of 980 nm NIR laser. Therefore, the amounts of green light photons generated by G-UP phosphor were much higher than those of blue and red lights photons by B-UP and R-UP phosphors, resulting in the highest photoactivity of (1:1)@G-UP/C-TiO₂ composite. From these results, it may be concluded that the NIR light induced photocatalytic performance was introduced via an up-conversion of NIR light to blue, green or red lights, which are reabsorbed by C-TiO₂ for photocatalysis.

In order to further understand the UV, visible and NIR lights utilization efficiency in the composites, the apparent photonic efficiency (ξ_λ) of the samples were calculated according to the equation [4,8,37,38]:

$$\xi_\lambda = \frac{(F_{NO} \times \alpha_\lambda)}{(P_\lambda \times S \times A_\lambda)} \quad (1)$$

Table 1

The calculated photonic efficiencies of the samples under the irradiation of different wavelengths of lights.

Photocatalyst	Photonic efficiency (%)				
	LED light 390 nm	LED light 445 nm	LED light 530 nm	LED light 627 nm	Infrared laser 980 nm
C-TiO ₂	0.36	0.43	0.61	0.26	0
(1:1)@B-UP/C-TiO ₂	0.28	0.32	0.40	0.47	3.83
(1:1)@G-UP/C-TiO ₂	0.31	0.36	0.42	0.49	4.50
(1:1)@R-UP/C-TiO ₂	0.28	0.30	0.37	0.42	1.61

where λ indicates the wavelength of the used irradiation lights (as shown in Fig. A.1, in which the intensity of lights has been normalized to the same order of magnitude), F_{NO} ($\mu\text{mol s}^{-1}$) the flow quantity of NO molecules in the reaction gas, α_λ (%) the deNO_x ability of the photocatalysts, P_λ ($\mu\text{mol m}^{-2} \text{s}^{-1}$) the photo number with the wavelength of light irradiated on the samples, S (m^2) the illuminated area and A_λ the absorption capability of sample at the irradiation wavelength. Taking NIR light induced deNO_x activity of (1:1)@G-UP/C-TiO₂ composite as an example, F_{NO} is $1.488 \times 10^{-4} \mu\text{mol s}^{-1}$ (NO, 1 ppm, 200 mL min^{-1}), α_λ 9.3% (as shown in Fig. 5(d)), P_λ $50.3 \mu\text{mol m}^{-2} \text{s}^{-1}$ and S $0.4 \times 10^{-4} \text{ m}^2$ (as display in Table. S1), A_λ 15.3% obtained from Fig. 3(b). Under these conditions, the calculated $\xi_{980\text{nm}}$ was about 4.5% and all of the calculated ξ_λ for the samples C-TiO₂, (1:1)@B-UP/C-TiO₂, (1:1)@G-UP/C-TiO₂, (1:1)@R-UP/C-TiO₂ under the irradiation of different wavelengths of lights were summarized in Table 1. It is apparent that the ξ_λ of NIR light responsive deNO_x ability of the composites showed the excellent values, which was much higher than those under UV and visible lights irradiation. This high ξ_λ for NIR light irradiation should be related to the poor NIR light absorption ability of the composites and the low energy of NIR light in comparison with those of UV and visible lights. Moreover, the green colour emitting up-conversion phosphor combined C-TiO₂ composite still presented the best ξ_λ value among three composites.

The effect of infrared light irradiation intensity on the deNO_x ability of typical (1:1)@G-UP/C-TiO₂ composite was also discussed as shown in Fig. A.4. It is clear that the NIR light induced deNO_x ability of the composite increased with increasing the light intensity of infrared laser, which further confirmed that the NIR light was truly active on the deNO_x ability of the composite photocatalysts.

As well known, the photostability was also one of the key points for practical application of photocatalysts. Fig. 6 shows the multi-cycles of deNO_x ability of the three composites irradiated by NIR light. After three runs testing, the photocatalytic activity of three composites did not change obviously, implying the good photostability of the up-conversion phosphors combined C-TiO₂ composites.

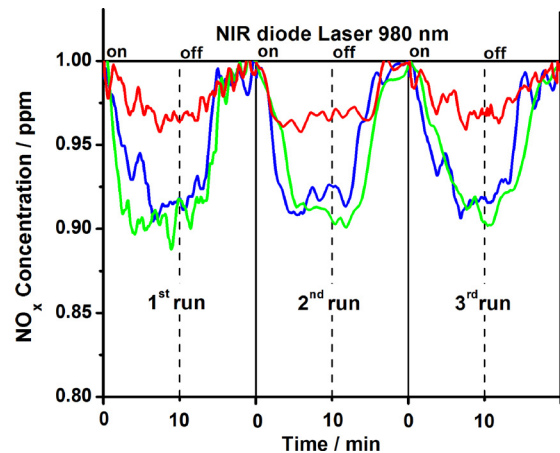


Fig. 6. Multi-cycle tests of deNO_x ability of (1:1)@B-UP/C-TiO₂, (1:1)@G-UP/C-TiO₂ and (1:1)@R-UP/C-TiO₂ composites under the irradiation of 980 nm light.

The degradation of RhB dye was also employed to evaluate the photocatalytic activity of samples in the solution system. Fig. 7 shows the RhB degradation capability of the samples under the irradiation of 980 nm infrared laser. All composites exhibited excellent NIR light induced RhB degradation activity, although uncoupled G-UP and C-TiO₂ showed no destruction ability. Additionally, the (1:1)@G-UP/C-TiO₂ represented the best RhB decomposition performance similar to that of deNO_x activity, following by (1:1)@B-UP/C-TiO₂ and (1:1)@R-UP/C-TiO₂ composites. Therefore, the up-conversion phosphors coupled C-TiO₂ composites possessed photocatalytic activities for not only destruction of NO_x gas but also dye degradation in solution under NIR lights irradiation.

Fig. 8 shows the possible mechanism of UV, visible and NIR lights responsive photocatalysis of the up-conversion phosphors coupled C-TiO₂ composites. It is well acknowledged that the function of up-conversion phosphors is to transfer long wavelength of

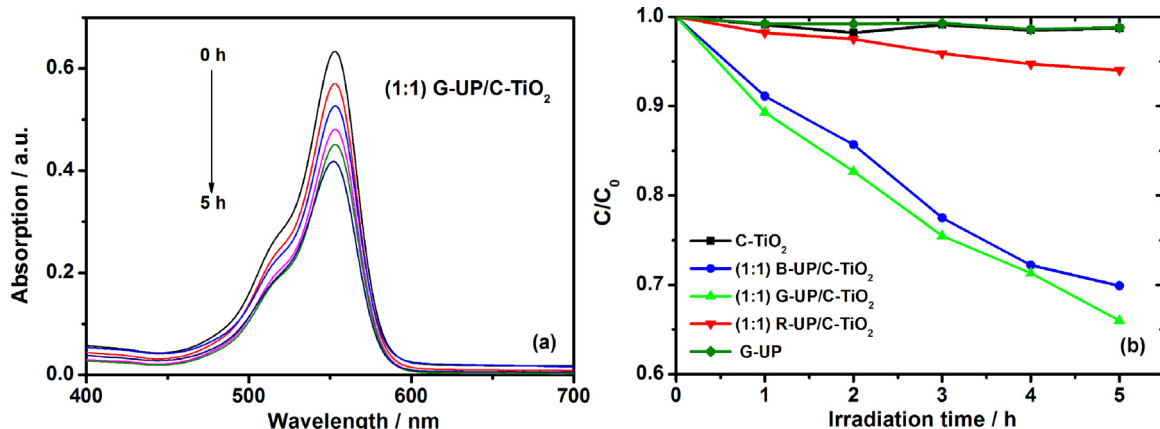


Fig. 7. Time change in the absorbance of RhB aqueous solution in the presence of (1:1)@G-UP/C-TiO₂ composite (a) and RhB degradation performance of samples C-TiO₂, (1:1)@B-UP/C-TiO₂, (1:1)@G-UP/C-TiO₂, (1:1)@R-UP/C-TiO₂ and G-UP (b) under the irradiation of 980 nm infrared laser.

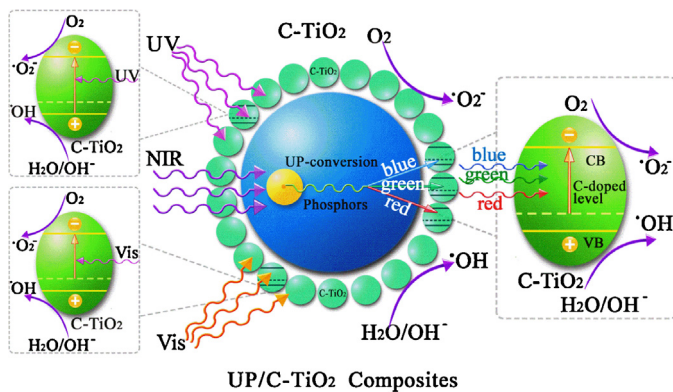


Fig. 8. The possible mechanism of UV, visible and NIR lights induced photocatalysis of up-conversion phosphors coupled C-TiO₂ composites. (For interpretation of the references to color in this figure legend, the reader is referred to the web version of this article.)

light (NIR light) to different short wavelengths of lights (UV, blue, green, red lights, etc.), achieving anti-stokes shift by a multi-photon mechanism [39]. When a NIR lights are irradiated to the present composites, the up-conversion phosphor would be excited, and then blue, green or red lights are emitted. The emitted visible lights could be absorbed by the C-TiO₂ in the composites, owing to the narrowed band gap of C-TiO₂ by C doping in O site of TiO₂ lattice (as shown in Fig. 3).

In this case, the electron could be excited from C doped levels to the conduction band of C-TiO₂. The photogenerated hole in the valence band would be further trapped by water and adsorbed OH⁻ species in the air to produce hydroxyl radicals •OH. In addition, the photoexcited electron in the conduction band would also react with absorbed oxygen to generate •O₂⁻. Finally, the target nitrogen monoxide could be oxidized by these reactive oxygen radicals, hydroxyl radicals, molecular oxygen, and water in the air to produce HNO₂ or HNO₃. These reaction process has been investigated by many researchers as presented in the following equations: [27,40,41]



As for UV and visible lights irradiation, these two lights could be directly absorbed by C-TiO₂ in the composites to take place the photocatalytic process. Therefore, the up-conversion phosphors coupled C-TiO₂ composites fabricated in the present work was feasible to be excited by UV, visible and NIR lights simultaneously, finally producing corresponding high performance of photocatalytic activities.

4. Conclusions

The blue, green, red colour emitting up-conversion phosphors coupled C-TiO₂ composites have been successfully prepared by a facile calcination assisted solvothermal method. The DRS and PL data demonstrated that after combining C-TiO₂ photocatalyst with up-conversion phosphors, the composites could be excited by UV, visible and NIR lights simultaneously. Furthermore, the absorbed NIR light by composites could be up-converted to blue, green or red lights, being reabsorbed by C-TiO₂ in composites. More importantly, the up-conversion phosphors coupled C-TiO₂ composites presented excellent continuous NO gas destruction ability under the irradiation of weak UV, visible and NIR lights along with

good photostability. According to the calculated photonic efficiency about photocatalytic activity, the NIR light induced deNO_x ability of composites illustrated the highest photonic efficiency value compared with those of UV and visible lights responsive ones. Meanwhile, the green colour emitting up-conversion phosphors coupled C-TiO₂ composite exhibited higher deNO_x capability than blue and red colour emitting ones, especially for NIR light induced photoactivity, owing to the higher emission efficiency of green up-conversion phosphor. Besides, the composites also displayed nice NIR light induced photocatalytic activity for RhB dye degradation in solution.

Acknowledgements

This research was supported in part by the Management Expenses Grants for National Universities Corporations from the Ministry of Education, Culture, Sports, Science for Technology of Japan (MEXT), the TAGEN Project 2013 in Tohoku University, the Adaptable and Seamless Technology Transfer Program through Target-driven R&D, JST (AS251Z00155M), and Hatano Foundation in IMRAM, Tohoku University.

Appendix A. Supplementary data

Supplementary data associated with this article can be found, in the online version, at <http://dx.doi.org/10.1016/j.apcatb.2014.03.028>.

References

- [1] S. Livraghi, M.C. Paganini, E. Giamello, A. Selloni, C. Divalentin, G. Pacchioni, *J. Am. Chem. Soc.* 128 (2006) 15666–15671.
- [2] M. Gratzel, *Nature* 414 (2001) 338–344.
- [3] J. Wang, S. Yin, Q. Zhang, F. Saito, T. Sato, *J. Mater. Chem.* 13 (2003) 2348–2352.
- [4] H.H. Li, S. Yin, T. Sato, *Appl. Catal., B* 106 (2011) 586–591.
- [5] C. Chen, M.C. Long, H. Zeng, W.M. Cai, B.X. Zhou, J.Y. Zhang, Y.H. Wu, D.W. Ding, D.Y. Wu, *J. Mol. Catal. A: Chem.* 314 (2009) 35–41.
- [6] T.F. Long, X.L. Dong, X.W. Liu, J.X. Liu, S. Yin, T. Sato, *Res. Chem. Intermed.* 36 (2010) 61–67.
- [7] A.K. Bhattacharya, K.K. Mallick, A. Hartridge, *Mater. Lett.* 30 (1997) 7–13.
- [8] S. Yin, B. Liu, P.L. Zhang, T. Morikawa, K. Yamamoto, T. Sato, *J. Phys. Chem. C* 112 (2008) 12425–12431.
- [9] S.U.M. Khan, M. Al-Shahry, W.B. Ingler Jr., *Science* 297 (2002) 2243–2245.
- [10] S. Yin, Q. Zhang, F. Saito, T. Sato, *Chem. Lett.* 32 (2003) 358–359.
- [11] S. Yin, H. Hasegawa, D. Maeda, M. Ishitsuka, T. Sato, *J. Photochem. Photobiol., A* 163 (2004) 1–8.
- [12] X.B. Chen, L. Liu, P.Y. Yu, S.S. Mao, *Science* 331 (2011) 746–750.
- [13] J.H. Wu, Z. Lan, J.M. Lin, M.L. Huang, S.C. Hao, T. Sato, S. Yin, *Adv. Mater.* 19 (2007) 4006–4011.
- [14] D. Duonghong, E. Borgarello, M. Gratzel, *J. Am. Chem. Soc.* 103 (1981) 4685–4690.
- [15] S.H. Hwang, C.H. Kim, J.S. Jang, *Catal. Commun.* 12 (2011) 1037–1041.
- [16] R.Y. Liu, P.G. Hu, S.W. Chen, *Appl. Surf. Sci.* 258 (2012) 9805–9809.
- [17] T. Ohno, F. Tanigawa, K. Fujihara, *J. Photochem. Photobiol., A* 127 (1999) 107–110.
- [18] R. Asahi, T. Morikawa, T. Ohwaki, K. Aoki, Y. Taga, *Science* 293 (2001) 269–271.
- [19] S. Yin, M. Komatsu, Q.W. Zhang, F. Saito, T. Sato, *J. Mater. Sci.* 42 (2007) 2399–2404.
- [20] S. Obregón, G. Colón, *Chem. Commun.* 48 (2012) 7865–7867.
- [21] Y.N. Tang, W.H. Di, X.S. Zhai, R.Y. Yang, W.P. Qin, *ACS Catal.* 3 (2013) 405–412.
- [22] W.P. Qin, D.S. Zhang, D. Zhao, L.L. Wang, K.Z. Zheng, *Chem. Commun.* 46 (2010) 2304–2306.
- [23] C.H. Li, F. Wang, J. Zhu, J.C. Yu, *Appl. Catal., B* 100 (2010) 433–439.
- [24] W. Wang, W.J. Huang, Y.R. Ni, C.H. Lu, L.J. Tan, Z.Z. Xu, *Appl. Surf. Sci.* 282 (2013) 832–837.
- [25] Z.J. Zhang, W.Z. Wang, J. Xu, M. Shang, J. Ren, S.M. Sun, *Catal. Commun.* 13 (2011) 31–34.
- [26] X.Y. Wu, S. Yin, Q. Dong, B. Liu, Y.H. Wang, T. Sekino, S.W. Lee, T. Sato, *Sci. Rep.* 3 (2013) 2918.
- [27] X.Y. Wu, S. Yin, Q. Dong, C.S. Guo, H.H. Li, T. Kimura, T. Sato, *Appl. Catal., B* 142–143 (2013) 450–457.
- [28] S. Heer, K. Kompe, H.U. Gudel, M. Haase, *Adv. Mater.* 16 (2004) 2102–2105.
- [29] Y.J. Sun, Y. Chen, L.J. Tian, Y. Yu, X.G. Kong, J.W. Zhao, H. Zhang, *Nanotechnology* 18 (2007) 275609–275617.
- [30] B. Neumann, P. Bogdanoff, H. Tributsch, S. Sakthivel, H. Kisch, *J. Phys. Chem. B* 109 (2005) 16579–16586.

- [31] X. Wang, S. Meng, X. Zhang, H. Wang, W. Zhong, Q. Du, *Chem. Phys. Lett.* 444 (2007) 292–296.
- [32] X.Y. Wu, S. Yin, Q. Dong, C.S. Guo, T. Kimura, J. Matsushita, T. Sato, *J. Phys. Chem. C* 117 (2013) 8345–8352.
- [33] C.D. Valentin, G. Pacchioni, A. Selloni, *Chem. Mater.* 17 (2005) 6656–6665.
- [34] X.W. Cheng, X.J. Yu, Z.P. Xing, L.S. Yang, *Int. J. Photoenergy* 2012 (2012) 1–6.
- [35] R. Quesada-Cabrera, A. Mills, C. O'Rourke, *Appl. Catal., B* 150–151 (2014) 338–344.
- [36] S. Yin, M. Komatsu, Q. Zhang, T. Sato, *J. Mater. Sci.* 42 (2004) 2399–2404.
- [37] H.H. Li, S. Yin, Y.H. Wang, T. Sato, *J. Catal.* 286 (2012) 273–278.
- [38] S. Obregón, A. Kubacka, M. Fernández-García, G. Colón, *J. Catal.* 299 (2013) 298–306.
- [39] J.C. Boyer, F. van Veggel, *Nanoscale* 2 (2010) 1417–1419.
- [40] Z.H. Ai, W.K. Ho, S.C. Lee, L.Z. Zhang, *Environ. Sci. Technol.* 43 (2009) 4143–4150.
- [41] Y. Ohko, Y. Nakamura, A. Fukuda, S. Matsuzawa, K. Takeuchi, *J. Phys. Chem. C* 112 (2008) 10502–10508.